Geomechanics and Engineering, *Vol. 25, No. 2 (2021) 99-109*
DOI: https://doi.org/10.12989/gae.2021.25.2.099

Three-dimensional finite element analysis of urban rock tunnel under static loading condition: Effect of the rock weathering

Mohammad Zaid*

Department of Civil Engineering, Zakir Husain College of Engineering and Technology, Aligarh Muslim University, Aligarh, U.P., Pin 202002, India

(Received January 25, 2021, Revised March 24, 2021, Accepted March 29, 2021)

Abstract. Tunnel provide faster, safer and convenient way of transportation for different objects. The region where it is construction and surrounding medium has significant influence on the overall stability and performance of tunnel. The present simulation has been carried out in order to understand the behaviour of rock tunnel under static loading condition. The present numerical model has been validated with the laboratory scaled model and field data of underground tunnels. Both lined and unlined tunnels have been considered in this paper. Finite element technique has been considered for the simulation of static loading effect on tunnel through Abaqus/Standard. The Mohr-Coulomb material model has been considered to simulate elastoplastic nonlinear behaviour of different rock types, i.e., Basalt, Granite and Quartzite. The four different stages of rock weathering are classified as fresh, slightly, moderately, and highly weathered in case of each rock type. Moreover, extremely weathered stage has been considered in case of Quartzite rock. It has been concluded that weathering of rock and overburden depth has great influence on the tunnel stability. However, by considering a particular weathering stage of rock for each rock type shows varying patterns of deformations in tunnel.

Keywords: rock; tunnel; basalt; granite; quartzite; static loading; Abaqus

1. Introduction

Tunnels and other underground structures have been considered as inseparable fundamental parts of modern metro cities. These structures satisfy different needs associated with transportation of goods and services such as in water canals, transportation tunnels, military caches, auxiliary tunnels, and shelters. In addition, due to rapid migration of people from rural to urban cities has increased the demand for faster and safer metro system. The metro tunnels in urban underground space have been constructed under high-rise building and therefore, these underground spaces experience varying overburden conditions. Moreover, presence of underground structures in and around border areas has utmost importance in country's defense system. Furthermore, scarcity of land for modernization of existing transportation system has attracted engineers and designers to adopted underground tunnels as better solution. Consequently, several studies related to underground tunnels were carried out to understand the effect of weathering, seismic loading, static loading, impact loading, blast loading and joint orientation (Gahoi *et al.* 2017, Naqvi *et al.* 2017, 2020, Ali Khan *et al.* 2019, Athar *et al.* 2019, Zaid *et al.* 2019a, b, 2020a, b, 2021, Zaid and Sadique 2020 a, d, b, c, Zaid and Rehan Sadique 2021, Zaid and Mishra 2021).

The tunnelling results in subsurface and surface settlement due to overlying superstructures, which has been studied in literature by several researchers. The effect of stratification and superstructural load has been studied by researchers in past (Khezri *et al.* 2016, Ali Khan *et al.* 2019, Naqvi *et al.* 2020). It was observed that simple elastic model in finite element technique overemphasizes the deformations in underground structures; therefore, elastoplastic material model should be considered in similar studies (Shahin *et al.* 2011). Plastic zones are found before failure therefore, the equations for calculating its occurrence and thickness was proposed by Komurlu *et al.* (2015). Liu *et al.* (2010) had presented a methodology for horse-shoe shape tunnels to calculate critical depth. Cross-section of tunnel plays an important role in governing design parameters, therefore, the plastic zone formation due to different forces and deformations was performed by Peila (1994). Moreover, tunnels can be categorised into shallow, deep and intermediate depending upon the overburden depth as suggested by Xu *et al.* (2000) and Ming-nian *et al.* (2010).

Properties of intact rock and in-situ condition of rockmass plays an important role in performance of tunnel boring machine (TBM). In case of different schistose rock, optimal thrust and revolutions of TBM were obtained by Eftekhari *et al.* (2018). The surface settlement and change in pore water pressure were observed by Wang *et al.* (2010), where maximum settlement was found in case of creep (71% of total settlement). They suggested that settlement due to creep can be reduced by installing a rigid concrete lining. Ground settlement in cohesionless soil can be calculated by available equations; nevertheless, these equations have limitations (Mazek 2014). Moreover, ground

*Corresponding author, M.Tech Student
E-mail: mohammadzaid1@zhcet.ac.in

http://www.techno-press.org/?journal=gae&subpage=7
ISSN: 2005-307X (Print), 2092-6219 (Online)

response curve for underwater tunnels was proposed by Fahimifar *et al.* (2015) through considering different loads. In addition, surface settlement can be reduced by using a layer of Geosynthetics under footing of structure (Rebello *et al.* 2018). Likewise, different researchers had studied the surface settlement due to tunnelling in varying conditions (Yang and Li 2017, Zheng *et al.* 2017, Kim *et al.* 2018, Rezaei *et al.* 2019). Twin-tunnel construction has increased the ideal usage of underground space; however, the forces in lining of initial tunnel are greatly affected by construction of second tunnel (Do *et al.* 2014a). Similar studies were carried out to understand different methods of twin tunnels by considering different factors associated with tunnels (Do *et al.* 2014b, Nawel and Salah 2015, La *et al.* 2018).

It has been found from the literature survey that study of tunnel under static loading were concentrated on surface settlement due to tunnel excavation. Moreover, empirical and analytical methods were used to study the behaviour of underground tunnels. Furthermore, previous researchers considered tunnels constructed in soil medium. However, number of underground urban tunnels are constructed in rocky/hilly regions of different parts of the world. Therefore, in the present study, an attempt has been made to understand the behavioral response of rock tunnel has been considered. In addition, effect of rock weathering due to different reasons has been considered through changes obtained in terms of physical and mechanical properties. Also, three different rocks, i.e. Basalt, Granite and Quartzite are considered in the present analysis. It has been observed that overburden depth also plays a pivotal role in tunnel stability; therefore, overburden depth has been varied for each stage of rock weathering. Correspondingly, both lined and unlined cases of tunnel are considered in the present simulation. A finite element technique has been considered for the present simulation, thus, Abaqus/Standard has been adopted.

2. Finite element analysis

The present paper deals with the study of urban underground tunnels, with or without lining, under static loading condition. The three different rocks, i.e. Basalt, Granite and Quartzite are considered with four weathering stages in each type of rock in order to analyze the effect of rock weathering. The input parameters are taken from Gupta (1997), where properties of different weathering stages were obtained through laboratory testing. A 3D finite element simulation has been carried out for the rock tunnel model having dimensions of 0.30 m x 0.30 m x 0.35 m. The present model of tunnel has been adopted based on the laboratory size presented by Zaid and Mishra (2021). The finite element analysis software Abaqus/Standard has been considered to carry out the present static loading simulation of rock tunnels (Hibbitt *et al.* 2014, Systemes 2014).

2.1 Geometry

The model has cross-section of 0.30 m x 0.30 m, and extruded up to the length of 0.35 m with varying overburden depth, geometry and meshed model has been shown in Figs. 1 and 2. The tunnel has 0.05 m diameter and lining thickness of 1.7×10^{-3} m (Zaid *et al.* 2020a, Zaid and Mishra 2021). The overburden depth has been varied to understand the effect of overburden depth in different weathering stages of rock. Three different overburden depths have been considered in the present study are 0.025 m, 0.035 m and 0.05 m.

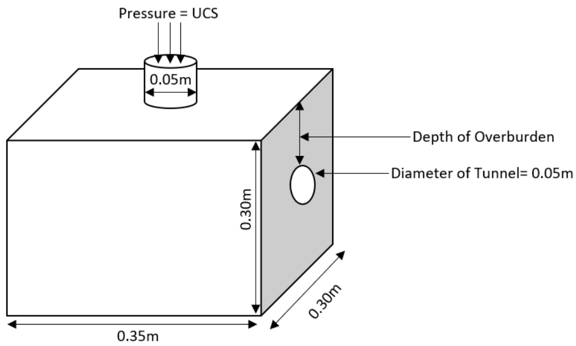

Fig. 1 Geometry of model

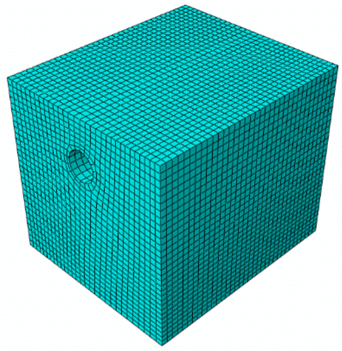

Fig. 2 Meshing of the model

2.2 Properties of materials

The Mohr-Coulomb constitutive model has been adopted for different weathering stages of rocks in present simulation. There are three different rocks, i.e., Basalt, Granite and Quartzite adopted for the analysis. Four different stages of weathering for each rock-type has been considered, i.e., Fresh (1), Slightly Weathered (2), Medium Weathered (3), and Highly Weathered (4), but in case of Quartzite rock, fifth stage of weathering i.e., Extremely Weathered (5) rock has also been added. The elastoplastic material properties of different rocks along with their weathering stages are shown in Table 1.

The yield criterion of Mohr-Coulomb plasticity model is given by

$$\tau = c + \sigma \tan \phi \tag{1}$$

where- shear stress, cohesion, normal stress and internal friction angle are represented by τ, c, σ and ϕ respectively.

For the 3D model of rock surrounding the tunnel opening, the base has fixed and sides have roller support boundary condition. A patch has been placed at the center of tunnel length on ground having 0.05 m in diameter and

Table 1 Input parameters of different rocks for the present simulation (Gupta 1997)

Rock Type	Density (kg/m^3)	Young's Modulus (GPa)	Poisson's Ratio	Cohesion (MPa)	Angle of Friction	UCS (MPa)
Quartzite						
Fresh	2680	93.75	0.185	27.13	65.30	207.03
Slightly Weathered	2590	51.14	0.185	26.24	57.33	125.60
Medium Weathered	2500	16.07	0.223	20.11	54.52	60.60
Highly Weathered	2420	12.18	0.213	15.75	49.49	32.20
Extremely Weathered	2200	1.86	0.394	4.80	44.06	12.40
Granite						
Fresh	2750	36.84	0.187	25.23	58.32	132.80
Slightly Weathered	2690	19.46	0.208	22.67	52.16	102.70
Medium Weathered	2540	12.99	0.250	10.55	48.34	53.01
Highly Weathered	1970	0.36	0.250	1.36	44.30	2.54
Extremely Weathered	2750	36.84	0.187	25.23	58.32	132.80
Basalt						
Fresh	2960	46.51	0.187	26.25	63.38	172.55
Slightly Weathered	2790	20.63	0.260	18.50	53.71	93.20
Medium Weathered	2560	2.77	0.272	8.08	43.87	17.80
Highly Weathered	2120	0.63	0.272	1.64	33.33	3.40
Extremely Weathered	2960	46.51	0.187	26.25	63.38	172.55

height. It has been loaded in the form of pressure equal to the unconfined compressive strength (UCS) of surrounding rock type. Initially, pressure was equal to 100% value of UCS, i.e., 0% reduction, later it was decreased by 10% in each subsequent case until 90% reduction in UCS. General hard contact and penalty contact has been provided between different parts of the model. C3D8R type of mesh element has been provided in all the cases. The mesh convergence and boundary convergence study were performed as presented by Zaid and Mishra (2021) where, further details related to element size and meshing were also presented.

2.3 Stages of analysis

In the present simulation of static loading in case of rock tunnel has been carried out by following steps involved in modelling and analysis using Abaqus that describe the procedure for carrying out present simulation i.e.,

• Initially, geometry of the model, having dimensions as mentioned earlier, has been created in Abaqus/CAE module of Abaqus. Geometry of all parts involved in the analysis were created.

• Afterwards, property was assigned to each part in property module, properties of material already present in property directory were imported, however, if not available in directory, and then new property was created and exported to directory.

• In next step i.e., assembly module, rock surrounding a tunnel opening, lining and loading patch were assembled by using instance tools for moving and rotating.

• Additionally, a step was created to define static loading condition, where Static-General step was selected with total time as 1 and, initial & maximum increment was also 1 (unit-less).

• Further, interaction between different parts of the model was assigned by creating interaction property from corresponding manager.

• In load module, the base of the tunnel was restrained in all directions and the patch has been loaded with pressure equal to the value of UCS of surrounding rock type. Moreover, the sides were assigned roller support.

• In the last step of modelling, meshing of each part was carried out and assigned C3D8R element type. The meshing of tunnel, lining and patch has been adopted as 2 mm, 1 mm and 0.5 mm respectively after carrying out mesh convergence study. Later, a job was created by naming a file and analysis for submitted.

3. Validation of static loading on tunnel

3.1 Validation for static loading with field data

The validation of static load on underground tunnel has been carried out by considering Greater Cairo metro Tunnel-Line 3, where field data of 9.1m diameter tunnel has been compared with simulation data of present technique as shown in Fig. 3. The geometry, boundary conditions and properties of geomaterial surrounding the tunnel opening has been kept constant as adopted by Mazek and Almannaei (2013). The tunnel is surrounded by stratified soil profile having five layers and water table is present at 2-4m below ground. It has been observed that the field data and results obtained by the present finite element technique are in close proximity. Therefore, simulation technique has been validated to carry out present analysis for rock tunnels

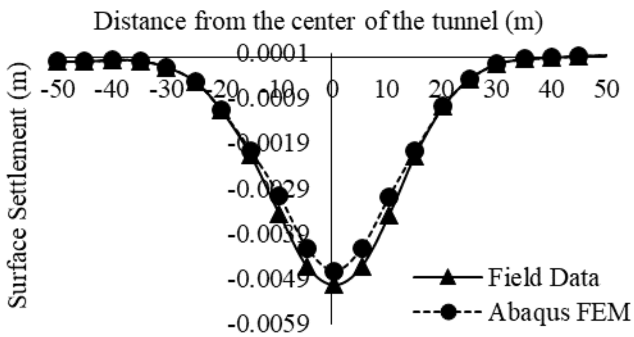

Fig. 3 Validation of numerical data with Field data

Table 2 Validation for static loading (Mishra 2019, Zaid and Mishra 2021)

Parameter	Geomaterial		POP	
	Experimental Study	Present Study	Experimental Study	Present Study
Crack length along the tunnel axis (mm)	97.00	93.00	85.00	81.00
Crack length transverse to the tunnel axis (mm)	41.00	40.00	34.00	31.00
Crown Deformation (mm)	0.37	0.38	0.30	0.28

under static loading.

3.2 Validation with laboratory data

Furthermore, presented technique of simulation has been adopted to compare results with data obtained from laboratory experimental testing (Mishra 2019). Where, a small scaled model was considered with 0.30 m x 0.30 m x 0.35 m dimensions and 0.05 m diameter of tunnel opening. Also, overburden depth of 0.05 m was considered in both experiment and Abaqus simulation. Moreover, parameters related to geometry, property and so on has been kept constant as adopted by Mishra (2019), Zaid and Mishra (2021). The results obtained by experimental testing and Abaqus simulation are presented in Table 2.

4. Results and discussion

In the present study, the finite element analysis has been carried out for the urban rock tunnels, using finite element software Abaqus/Standard. Three different rocks having four different weathering stages are considered for Basalt, Granite and Quartzite rocks, which represents rocks of different areas of Indian subcontinent. Generally, Basalt rock tunnels are found in the areas of Mumbai, Quartzite rock tunnels are usually encountered in New Delhi region and Granite rock tunnels are found in the region of Kolkata. The results of the parametric numerical analysis are discussed to understand static stability of rock tunnels. The effect of overburden depth has been taken into account along with the effect of weathering on rock. The results are compared in terms of deformation and stresses resulted due to static loading.

Deformation contours of different lined rock tunnels having 0.05 m diameter and 0.035 m overburden depth when subjected to load in the form of pressure equal to the value of UCS of surrounding rock are shown in Fig. 4. The maximum deformation observed in the present case of Fresh Basalt, Slightly Weathered Basalt, Medium Weathered Basalt, Highly Weathered Basalt, Fresh Granite, Slightly Weathered Granite, Medium Weathered Granite, Highly Weathered Granite, Fresh Quartzite, Slightly Weathered Quartzite, Medium Weathered Quartzite, Highly Weathered Quartzite, and Extremely Weathered Quartzite rock is 0.141 mm, 0.199 mm, 0.245 mm, 0.249 mm, 0.141 mm, 0.161 mm, 0.290 mm, 0.317 mm, 0.092 mm, 0.109 mm, 0.112 mm, 0.160 mm and 0.206 respectively. Therefore, Fresh Quartzite rock tunnel found to be safer and Highly Weathered Granite rock tunnel has maximum deformation, thus, the rock tunnels constructed in Highly Weathered Granite found to be susceptible to severe damage in comparison to rest of the rock tunnels considered in the present study.

Fig. 5 shows the effect of overburden depth for Highly Weathered Granite lined rock tunnel. Maximum deformation has been observed as 0.354 mm, 0.317 mm and 0.259 mm for 0.025 m, 0.035 m and 0.05 m overburden depth respectively. Therefore, as the overburden on the tunnel increases, it increases the safety of the tunnel. The reason behind the stability of tunnel with increase in overburden depth is due to result in lithostatic condition.

Fig. 6 shows the deformation versus percentage decrease in UCS for different rock in case of lined tunnels, having 0.025m overburden depth. Highly Weathered Granite, Extremely Weathered Quartzite, Medium Weathered Basalt, Fresh Basalt, Fresh Quartzite rock tunnels follows linear pattern for deformation corresponding to percentage decrease in Unconfined Compressive Strength and the rest rocks follows non-linear pattern. The deformation experienced by Highly Weathered/ Extremely Weathered rocks has maximum deformation and fresh rock having no effect of weathering has minimum deformation. For unlined tunnels, Fig. 7 shows similar pattern of deformation as shown in Fig. 6 for lined tunnels.

The deformation profile of different rock tunnels having lining has been shown in Fig. 8. The deformation profile has been plotted for the longitudinal deformation of the tunnel when subjected to static loading. The central part of the longitudinal length of tunnel experiences maximum deformation and the deformation diminishes along the length outward. The deformation profile has been plotted for 0.025 m overburden depth on tunnel having 0.05 m diameter. Highly Weathered Basalt has the maximum deformation at the central loading, where load has been applied.

The deformation profiles along the transverse direction has been plotted for all the rocks considered in the study having different zones of deformation encountered along the longitudinal direction of tunnel have been shown in Fig. 9. The zones of deformation taken into account in different rocks are Zone 1, Zone 2, Zone 3 and Zone 4. Current case considers 0.025m of overburden depth. Deformation zones along transverse direction were plotted for Fresh Basalt,

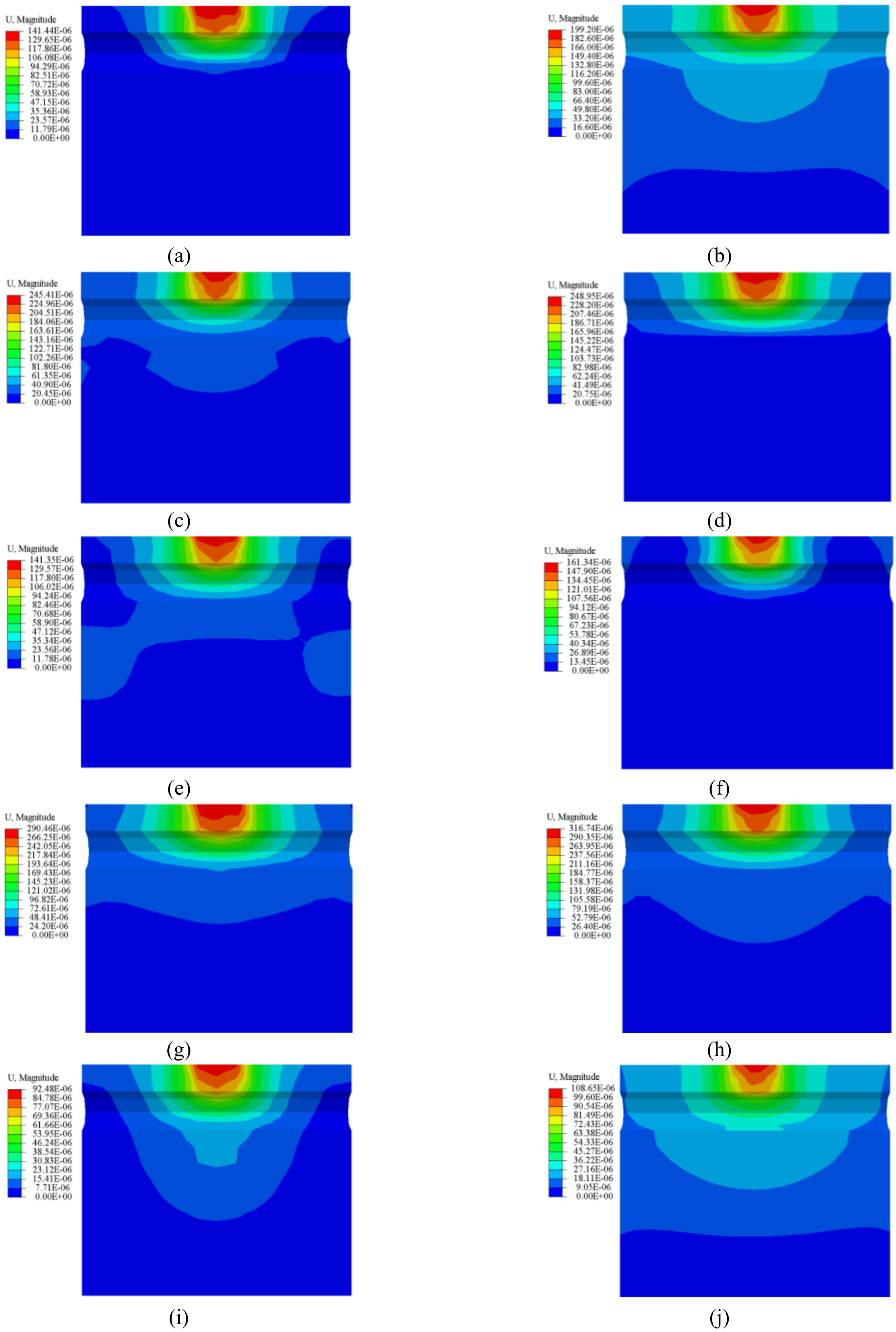

Fig. 4 Deformation (meters) contours of different rocks for lined tunnel having 0.035 cm overburden under 0% reduction in UCS, where (a) Fresh Basalt, (b) Slightly Weathered Basalt, (c) Medium Weathered Basalt, (d) Highly Weathered Basalt, (e) Fresh Granite, (f) Slightly Weathered Granite, (g) Medium Weathered Granite, (h) Highly Weathered Granite, (i) Fresh Quartzite, (j) Slightly Weathered Quartzite, (k) Medium Weathered Quartzite, (l) Highly Weathered Quartzite and (m) Extremely Weathered Quartzite rock

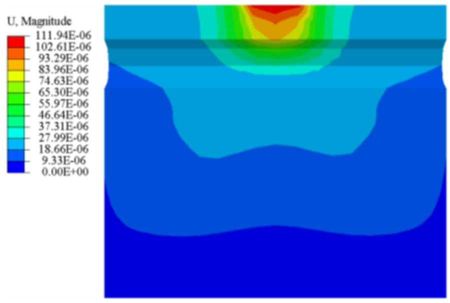

(k)

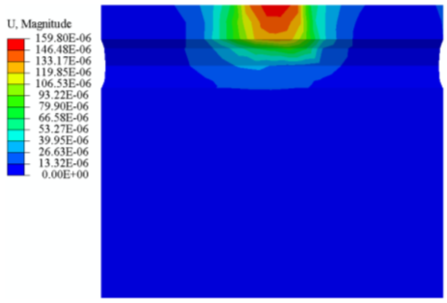

(l)

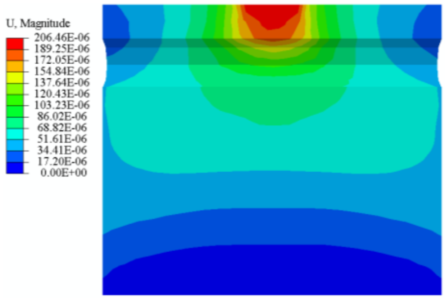

(m)

Fig. 4 Continued

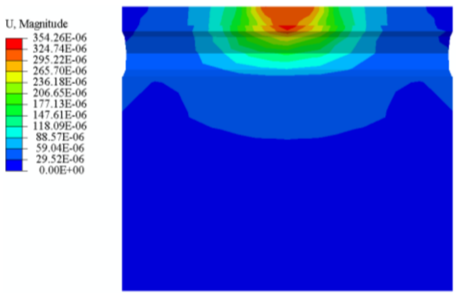

(a)

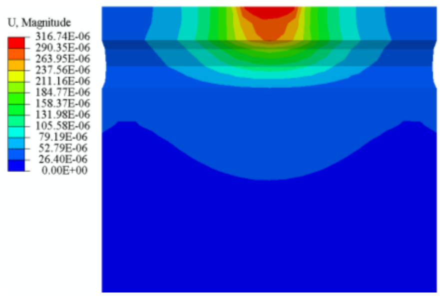

(b)

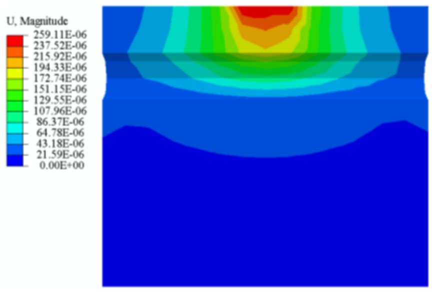

(c)

Fig. 5 Effect of Overburden Depth in case of Highly Weathered Granite in lined tunnel, (a) 2.5cm, (b) 3.5cm, and (c) 5cm overburden depth

Slightly Weathered Basalt, Medium Weathered Basalt, Highly Weathered Basalt, Fresh Granite, Slightly Weathered Basalt, Medium Weathered Basalt, Highly Weathered Basalt, Fresh Quartzite, Slightly Weathered Quartzite, Medium Weathered Quartzite, Highly Weathered Quartzite and Extremely Weathered Quartzite. Zone 1 lies at the center of the tunnel and hence, experiences maximum deformation, hence while moving away from the center the deformation decreases and dies out. Zone 4 represents the outer most profile of the rock tunnel deformation in transverse direction and it has minimum deformations in each case of rock tunnel considered. Zone 2 and Zone 3 are two intermediate profiles which shows transverse deformation profiles of rock tunnels while moving from maximum deformation to minimum deformation.

Table 3 represents mises stresses values for the comparison of effect of weathering and variation of load in the form of pressure, value of which has been taken equal to the value of UCS of surrounding rock. The value of UCS has been varied at an interval of 10% up to 90%. The effect of variation in the value of UCS also has been shown in Table 2. Fresh rock of each category of rocks i.e., Basalt,

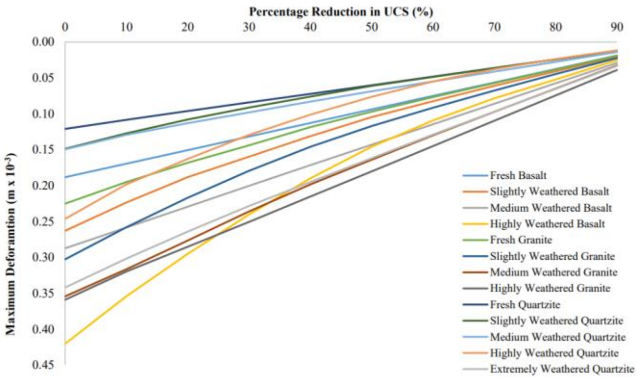

Fig. 6 Variation of deformation with percentage reduction in UCS for 2.5 cm overburden depth of lined tunnel

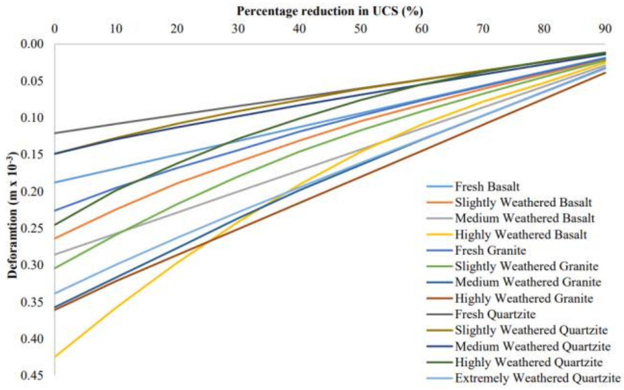

Fig. 7 Variation of deformation with percentage reduction in UCS for 0.025 cm overburden depth of unlined tunnel

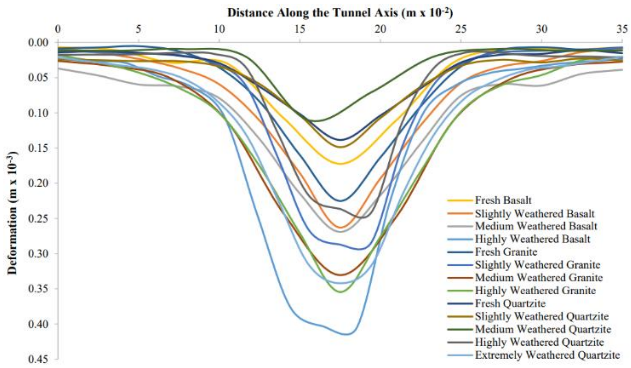

Fig. 8 Deformation profile of different rocks along the longitudinal axis of the tunnel having 0.025 m overburden for lined tunnel of 0.050 m diameter

Table 3 Comparison of Mises Stresses (in MPa) in different rocks with decrease in UCS

Type of Rock	Percentage of UCS Decreased									
	0%	10%	20%	30%	40%	50%	60%	70%	80%	90%
Basalt										
Fresh	226.40	200.70	175.20	150.20	128.90	108.50	88.57	71.30	54.01	27.76
Slightly Weathered	106.60	95.96	28.54	77.03	68.53	60.53	50.73	39.48	28.54	13.09
Medium Weathered	21.19	19.69	18.21	16.82	15.39	13.88	11.70	8.76	5.86	2.87
Highly Weathered	3.18	3.04	2.90	2.75	2.62	2.41	1.93	1.44	0.96	0.48
Granite										
Fresh	186.20	167.60	150.60	133.70	117.70	101.40	86.62	69.76	47.47	24.62
Slightly Weathered	140.50	128.40	116.30	104.80	106.60	80.70	66.48	51.93	37.13	16.45
Medium Weathered	38.92	35.82	32.82	30.03	27.13	23.87	20.09	15.92	12.21	5.65

Table 3 Continued

Type of Rock	Percentage of UCS Decreased									
	0%	10%	20%	30%	40%	50%	60%	70%	80%	90%
Granite										
Highly Weathered	3.75	3.49	3.22	2.96	2.69	2.24	1.80	1.35	0.91	0.46
Quartzite										
Fresh	219.70	193.40	169.50	148.10	120.90	96.92	76.90	60.50	45.62	26.00
Slightly Weathered	152.80	138.00	122.50	109.20	96.00	83.45	71.00	57.60	38.52	18.86
Medium Weathered	73.09	67.41	61.46	54.69	47.85	40.64	33.44	27.46	23.14	8.62
Highly Weathered	38.27	34.83	31.38	28.04	24.83	20.88	16.36	12.29	5.93	4.98
Extremely Weathered	6.14	5.52	5.24	5.10	4.82	4.53	4.49	4.01	2.69	1.37

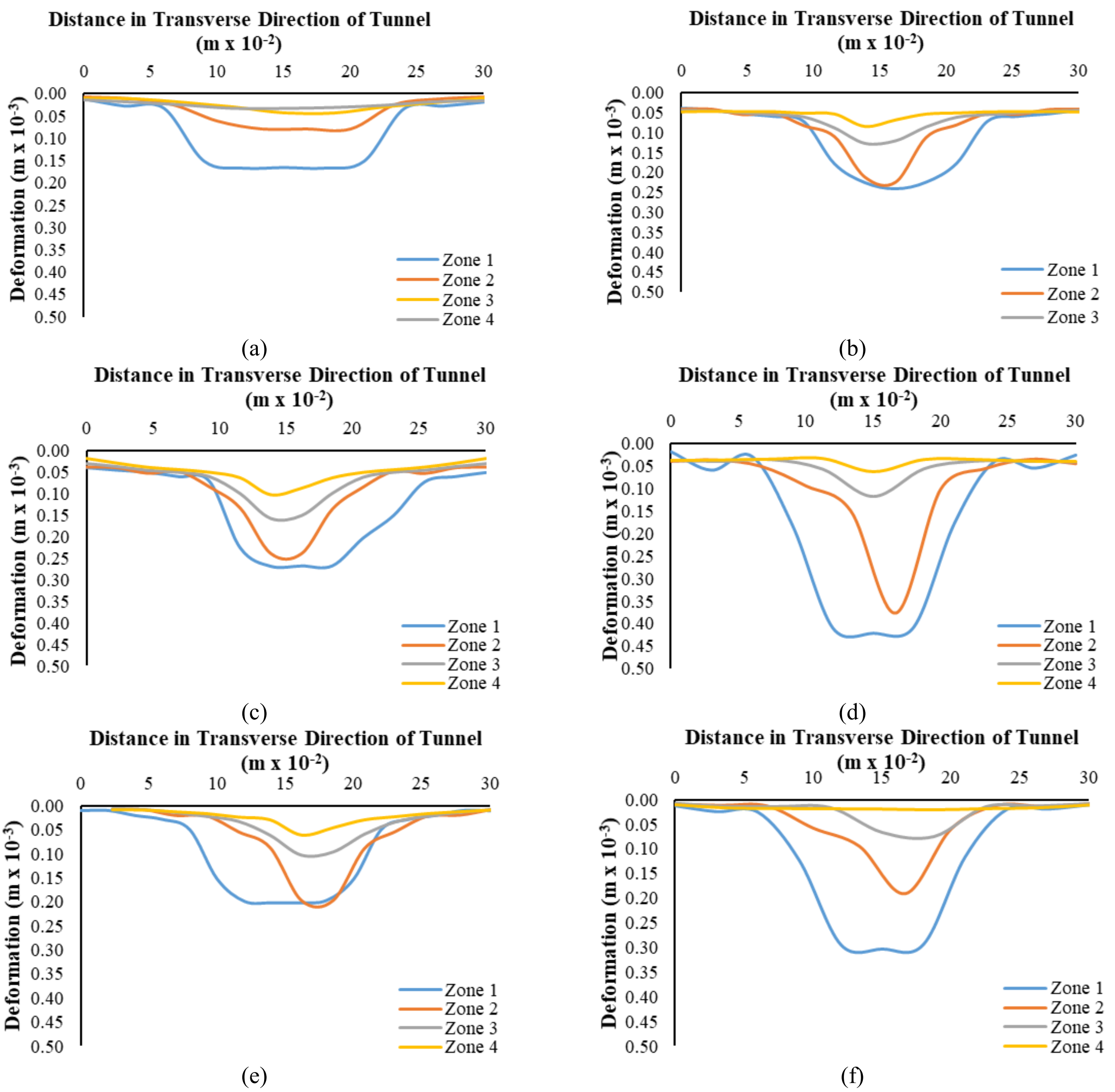

Fig. 9 Graphs for different deformation zones in various rocks for unlined tunnel having 0.025m overburden depth, (a) Fresh Basalt, (b) Slightly Weathered Basalt, (c) Medium Weathered Basalt, (d) Highly Weathered Basalt, (e) Fresh Granite, (f) Slightly Weathered Basalt, (g) Medium Weathered Basalt, (h) Highly Weathered Basalt, (i) Fresh Quartzite, (j) Slightly Weathered Quartzite, (k) Medium Weathered Quartzite, (l) Highly Weathered Quartzite and (m) Extremely Weathered Quartzite

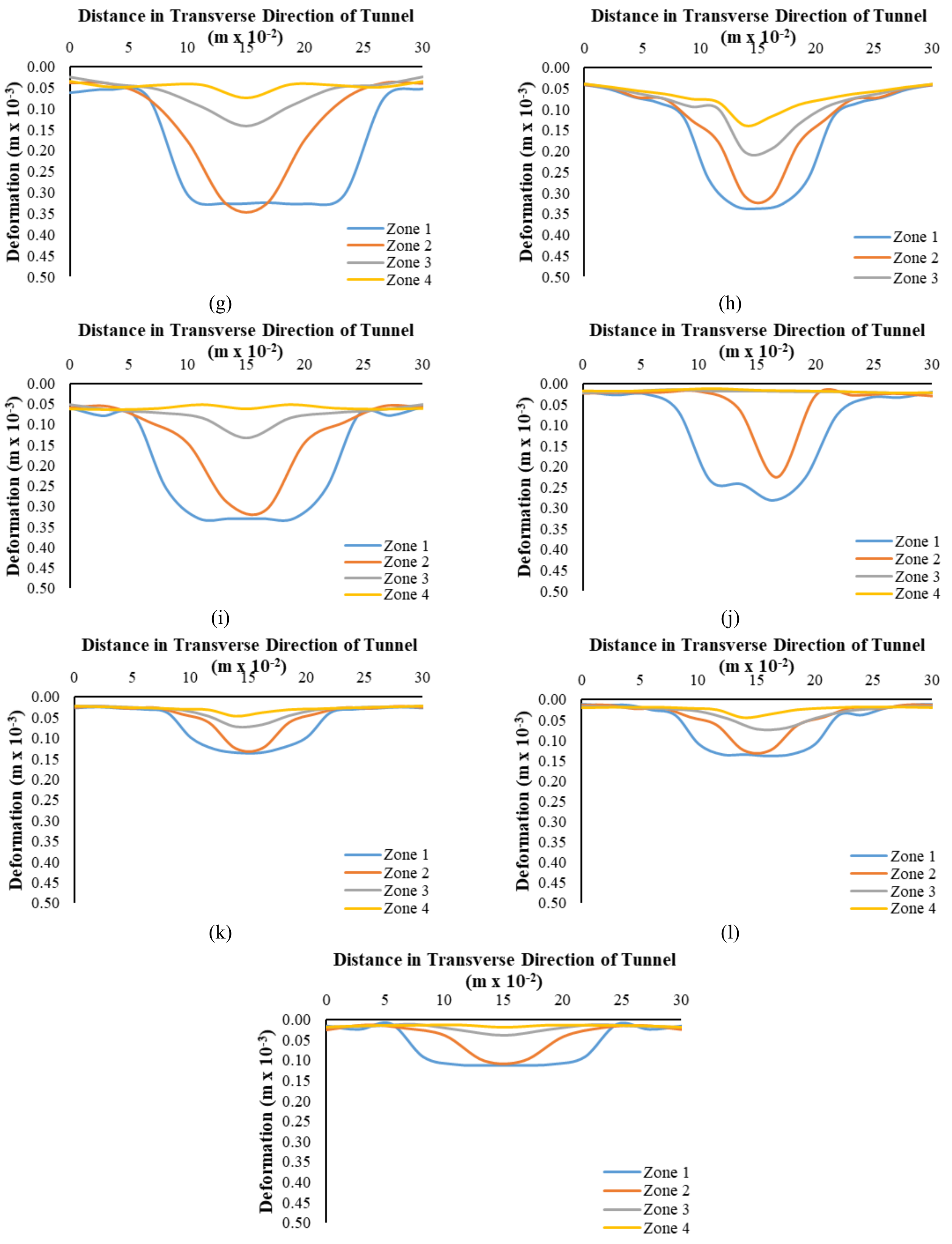

(g) (h) (i) (j) (k) (l) (m)

Fig. 9 Continued

Granite and Quartzite experiences maximum stress and the stress decreases with the effect of weathering on the rocks. Also, stress decreases with decrease in the value of UCS. Therefore, weathering has significant effect on the stability of shallow tunnels under static loading and substantial change has been observed in stress as the rock reaches to its highly/ extremely weathered stage from its fresh state.

5. Conclusions

The present simulation of static loading effect on rock tunnels with varying overburden depth and weathering stages in rock has been carried out using Abaqus. Three different overburden depths are considered as 0.025m, 0.035m and 0.05m in case of each weathering stage corresponding to different rocks i.e., Basalt, Granite and Quartzite. The load has been applied in the form of pressure, which has magnitude equal to the UCS of surrounding rock media. The magnitude of rock UCS has been varied from 0% to 90% reduction in terms of pressure magnitude. The four different rock weathering stages, i.e. fresh, slightly, medium and highly weathered stage, have shown that weathering of rock significantly causes damage under static loading.

It has been concluded that rockmass unaffected by weathering, i.e., fresh rock, shows significant strength against resisting superstructural load. However, slight weathering in rock surrounding the tunnel increases the magnitude of deformation and reduces the load resistance of tunnel. In addition, medium weathered and highly weathered rock has lowest degree of safety and therefore, require high strength tunnel lining material. Therefore, effect of weathering needs to be considered while tunnel design under the presence of static loading also.

In addition to weathering, overburden depth of tunnel has significant influence in dispersion of overcoming load from ground. In shallow depth tunnel, deformation/settlement has concentration in the tunnel corresponding to position of load. While, higher depth tunnels reduce the effect of overcoming load largely due to additional overburden depth. The magnitude of load has noteworthy role in behaviour of rock tunnels in different weathering stages. It has been concluded that effect of weathering in rock tunnel is significant when superstructural load has high magnitude. However, the deformation in tunnel has lesser variation due to weathering when lower magnitude load are considered.

References

Ali, K.M., Sadique, M.R. and Zaid, M. (2019), "Effect of stratification on underground opening: A numerical approach", *Adv. Transport. Eng.*, 133-142. https://doi.org/10.1007/978-981-13-7162-2_11.

Athar, M.F., Zaid, M. and Sadique, M.R. (2019), "Stability of different shapes of tunnels in weathering stages of basalt", *Proceedings of the National Conference on Advances in Structural Technology*, Silchar, Assam, India, February.

Dassault Systèmes (2014), *Abaqus 6.14 Documentation*, Dassault Systèmes, Providence, Rhode Island, U.S.A.

Do, N. A., Oreste, P., Dias, D., Antonello, C., Djeran-Maigre, I. and Livio, L. (2014b), "Stress and strain state in the segmental linings during mechanized tunnelling", *Geomech. Eng.*, **7**(1), 75-85. https://doi.org/10.12989/gae.2014.7.1.075.

Do, N.A., Dias, D., Oreste, P. and Djeran-Maigre, I. (2014a), "2D numerical investigations of twin tunnel interaction", *Geomech. Eng.*, **6**(3), 263-275. https://doi.org/10.12989/gae.2014.6.3.263.

Eftekhari, A., Aalianvari, A. and Rostami, J. (2018), "Influence of TBM operational parameters on optimized penetration rate in schistose rocks, a case study: Golab tunnel Lot-1, Iran", *Comput. Concrete*, **22**(2), 239-248. https://doi.org/10.12989/cac.2018.22.2.239.

Fahimifar, A., Ghadami, H. and Ahmadvand, M. (2015), "The ground response curve of underwater tunnels, excavated in a strain-softening rock mass", *Geomech. Eng.*, **8**(3), 323-359. https://doi.org/10.12989/gae.2015.8.3.323.

Gahoi, A., Zaid, M., Mishra, S. and Rao, K.S. (2017), "Numerical analysis of the tunnels subjected to impact loading", *Proceedings of the 7th Indian Rock Conference*, New Delhi, India, October.

Gupta, A.S. (1997), "Engineering behavior and classification of weathering rock", Ph.D. Dissertation, Indian Institute of Technology Delhi, Delhi, India

Hibbitt, D., Karlsson, B. and Sorensen, P. (2014), *ABAQUS User-Manual Release 6.14*, Dassault Systèmes Simulia Corporation, Providence, Rhode Island, U.S.A.

Khezri, N., Mohamad, H. and Fatahi, B. (2016), "Stability assessment of tunnel face in a layered soil using upper bound theorem of limit analysis", *Geomech. Eng.*, **11**(4), 471-492. https://doi.org/10.12989/gae.2016.11.4.471.

Kim, K., Lee, H., Kim, D., Choi, H. (2018), "Critical face pressure and backfill pressure in shield TBM tunneling on soft ground", *Geomech. Eng.*, **15**(3), 823-831. https://doi.org/10.12989/gae.2018.15.3.823.

Komurlu, E., Kesimal, A. and Hasanpour, R. (2015), "In situ horizontal stress effect on plastic zone around circular underground openings excavated in elastic zones", *Geomech. Eng.*, **8**(6), 783-799. https://doi.org/10.12989/gae.2015.8.6.783.

La, Y.S., Kim, B., Jang, Y.S. and Choi, W.H. (2018), "Stress interactions between two asymmetric noncircular tunnels", *Geomech. Eng.*, **15**(3), 869-877. https://doi.org/10.12989/gae.2018.15.3.869.

Liu, J.L., Wang, Z.Z. and Fang, X. (2010), "Formulas for computing geometry and critical depth of general horseshoe tunnels", *Trans. Amer. Soc. Agricult. Biol. Eng.*, **53**(4), 1159-1164. https://doi.org/10.13031/2013.32597.

Mazek, S.A. (2014), "Evaluation of surface displacement equation due to tunnelling in cohesionless soil", *Geomech. Eng.*, **7**(1), 55-73. https://doi.org/10.12989/gae.2014.7.1.055.

Mazek, S.A. and Almannaei, H.A. (2013), "Finite element model of Cairo metro tunnel-Line 3 performance", *Ain Shams Eng. J.*, **4**(4), 709-716. https://doi.org/10.1016/j.asej.2013.04.002.

Mishra, S. (2019), "Physical and numerical modeling of tunnels under impact and blast loads", Ph.D. Dissertation, Indian Institute of Technology Delhi, Delhi, India.

Naqvi, M.W., Akhtar, M.F., Zaid, M. and Sadique, M.R. (2020), "Effect of superstructure on the stability of underground tunnels" *Transport. Infrastruct. Geotechnol.*, 1-20. https://doi.org/10.1007/s40515-020-00119-6.

Naqvi, M.W., Zaid, M., Sadique, M.R. and Alam, M.M. (2017), "Dynamic analysis of rock tunnels considering joint dip angle: A finite element approach", *Proceedings of the 13th International Conference on Vibration Problems*, Assam, India, November-December.

Nawel, B. and Salah, M. (2015), "Numerical modeling of two parallel tunnels interaction using three-dimensional finite elements method", *Geomech. Eng.*, **9**(6), 775-791. https://doi.org/10.12989/gae.2015.9.6.775.

Peila, D. (1994), "A theoretical study of reinforcement influence on the stability of a tunnel face", *Geotech. Geol. Eng.*, **12**, 145-168. https://doi.org/10.1007/BF00426984.

Rebello, N.E., Shivashankar, R. and Sastry, V.R. (2018), "Surface displacements due to tunneling in granular soils in presence and absence of geosynthetic layer under footings", *Geomech. Eng.*, **15**(2), 739-744. https://doi.org/10.12989/gae.2018.15.2.739.

Rezaei, A.H., Shirzehhagh. M. and Golpasand, M.R.B. (2019), "EPB tunneling in cohesionless soils: A study on Tabriz Metro settlements", *Geomech. Eng.*, **19**(2), 153-165. https://doi.org/10.12989/gae.2019.19.2.153.

Shahin, H.M., Nakai, T., Zhang, F., Kikumoto, M. and Nakahara, E. (2011), "Behavior of ground and response of existing foundation due to tunneling", *Soils Found.*, **51**(3), 395-409. https://doi.org/10.3208/sandf.51.395.

Wang, M.N., Guo, J., Luo, L.S., Yu, Y., Yang, J.M. and Tan, Z.S. (2010), "Study of critical buried depth of large cross-section loess tunnel for high speed railway", *Rock Soil Mech.*, **31**, 1157-1162.

Wang, Z., Wong, R.C.K. and Heinz, H. (2010), "Assessment of long-term behaviour of a shallow tunnel in clay till", *Geomech. Eng.*, **2**(2), 107-123. https://doi.org/10.12989/gae.2010.2.2.107.

Xu, Z.M., Huang, R.Q. and Wang, S.T. (2000), "Tunnel classifying in light of depth", *Chin. J. Geol. Hazards Control*, **11**, 5-10.

Yang, X.L. and Li, W.T. (2017), "Reliability analysis of shallow tunnel with surface settlement", *Geomech. Eng.*, **12**(2), 313-326. https://doi.org/10.12989/gae.2017.12.2.313.

Zaid, M. and Mishra, S. (2021), "Numerical analysis of shallow tunnels under static loading: A finite element approach", *Geotech. Geol. Eng.*, 1-27. https://doi.org/10.1007/s10706-020-01647-1.

Zaid, M. and Sadique, M.R. (2020d), "Blast resistant behaviour of tunnels in sedimentary rocks", *Int. J. Protective Struct.* https://doi.org/10.1177/2041419620951211.

Zaid, M. and Sadique, M.R. (2020a), "Effect of unconfined compressive strength of rock on dynamic response of shallow unlined tunnel", *SN Appl. Sci.*, **2**(12), 1-13. https://doi.org/10.1007/s42452-020-03876-8.

Zaid, M. and Sadique, M.R. (2020b), "The response of rock tunnel when subjected to blast loading: Finite element analysis", *Eng. Reports*, **3**(2), e12293. https://doi.org/10.1002/eng2.12293.

Zaid, M. and Sadique, M.R. (2020c), "Numerical modelling of internal blast loading on a rock tunnel", *Adv. Comput. Des.*, **5**(4), 417-443. https://doi.org/10.12989/acd.2020.5.4.417.

Zaid, M. and Sadique, M.R. (2021), "Dynamic analysis of tunnels in western ghats of indian peninsula: Effect of Shape and Weathering", *Recent Trends Civ. Eng.*, 763-776. https://doi.org/10.1007/978-981-15-5195-6_57.

Zaid, M., Mishra, S. and Rao, K.S. (2019a), "Stability of different shapes of Himalayan tunnels under blast loading", *Proceedings of the 8th Indian Rock Conference*, New Delhi, India, November.

Zaid, M., Sadique, M.R. and Alam, M.M. (2021), "Blast analysis of tunnels in Manhattan-Schist and Quartz-Schist using coupled-Eulerian–Lagrangian method", *Innov. Infrastruct. Solutions*, **6**(2), 1-10. https://doi.org/10.1007/s41062-020-00446-0.

Zaid, M., Sadique, M.R., Alam, M.M. and Samanta, M. (2020b), "Effect of shear zone on dynamic behaviour of rock tunnel constructed in highly weathered granite", *Geomech. Eng.*, **23**(3), 245-259. https://doi.org/10.12989/gae.2020.23.3.245.

Zaid, M., Shah, I.A. and Farooqi, M.A. (2019b), "Effect of cover depth in unlined Himalayan tunnel: A finite element approach", *Proceedings of the 8th Indian Rock Conference*, New Delhi, India, November.

Zaid. M., Mishra, S. and Rao, K.S. (2020a), "Finite element analysis of static loading on urban tunnels", *Geotech. Characteriz. Modell.*, 807-823. https://doi.org/10.1007/978-981-15-6086-6_64.

Zheng, G., Du, Y., Cheng, X. and Deng, X. (2017), "Characteristics and prediction methods for tunnel deformations induced by excavations", *Geomech. Eng.*, **12**(3), 361-397. https://doi.org/10.12989/gae.2017.12.3.361.

CC